Eur. Phys. J. D (2018) 72: 215
https://doi.org/10.1140/epjd/e2018-80591-3

THE EUROPEAN PHYSICAL JOURNAL D

Regular Article

Influence of Al, Fe or Cu vapour on thermophysical properties of CO_2 plasmas

Yang Liu[1,a], Xiaohua Wang[1], Linlin Zhong[2], Aijun Yang[1], Mingzhe Rong[1], and Junhui Wu[3]

[1] State Key Laboratory of Electrical Insulation and Power Equipment, Xi'an Jiaotong University, No. 28 XianNing West Road, Xi'an, Shaanxi Province 710049, P.R. China
[2] School of Electrical Engineering, Southeast University, Nanjing 210096, P.R. China
[3] Pinggao Group Co. Ltd., Pingdingshan, Henan Province, 467001, P.R. China

Received 18 September 2017 / Received in final form 6 March 2018
Published online 18 December 2018

Abstract. CO_2 has been adopted by gas circuit breakers serving as an arc extinguishing gas and by arc welding as a shielding gas. These applications are usually accomplished by the erosion of metal constituting the device, which may modify arc properties. Therefore, this paper investigates the impact of metals (Al, Fe, Cu) on equilibrium compositions, thermodynamic (mass density, specific enthalpy and specific heat) and transport properties (thermal conductivity, viscosity and electrical conductivity) for CO_2 thermal plasmas, which are obtained using the Chapman–Enskog theory and the Gibbs free energy minimization method. Mass proportion is adopted for all mixtures. The presence of metals, particularly Al, can greatly enhance the electrical conductivity for CO_2, especially at low temperature even for a small concentration like 1%. Fe and Cu reveal quite close evolutions of electrical conductivity and present similar effects on electrical conductivity of CO_2 under the same mixing ratio. However, for viscosity and thermal conductivity of CO_2, the attenuating effects of metals, particularly Fe and Cu, are quite marginal with a concentration of 10%.

1 Introduction

CO_2 thermal plasma, or electrical arc, has been widely used in many industrial applications involving plasma cutting, surface treatment, arc welding and circuit breaker [1–4]. In metallurgical processes, CO_2 is used as shielding gas for gas metal arc welding to prevent the molten weld metal from contamination and for converter process to reduce the amount of converter dust; it is also used as a carrier and reacting gas in iron-making process. For electrical apparatus such as gas-insulated switchgears and high-voltage circuit breakers, CO_2 is considered as a promising alternative candidate of SF_6 gas for good electrical properties and environmental friendliness [5]. Moreover, CO_2 has been utilized as an insulation gas in high-voltage circuit breaker named LTA 72D1, developed by ABB Company [6].

In fact, the establishment of arc in above industrial applications usually is accomplished by the erosion of metal constituting the device. The existence of metallic vapour may modify dramatically the arc properties. For instance, in arc welding, Murphy found that the arc properties and the shape and size of weld pool were mainly affected by metal vapour [7]. Gonzalez et al. presented measurement on an Ar arc with an iron electrode and observed the cooling of arc temperature due to the existence of iron vapour [8]. Schnick et al. found that metal vapour can cause a cooling effect of the arc by increasing radiative emission coefficients [9]. In a circuit breaker, metal vapours from electrode and wall erosion, mixing with working gas, can affect arc characteristics. Zhang et al. [10] and Liau et al. [11] studied effects of copper vapour, released by electrode erosion, on arc characteristics in an SF_6 circuit breaker and found that copper vapour can lower arc core temperature and broaden arc radius. Lee et al. investigated both electrode evaporation and nozzle ablation processes in an SF_6 switchgear and observed higher electrical conductivity than that without considering copper erosion [12].

A further study or investigation of these thermal plasma processes usually utilizes various numerical models [13]. Moreover, the prerequisite to these numerical models requires the knowledge of corresponding thermal plasma properties. In order to better investigate arc behaviour and its extinction, these metallic vapours must be considered, which plays an essential role in more and more sophisticated numerical models. Therefore, before setting up numerical models, thermophysical properties considering metal vapours, for example, composition, thermodynamic and transport properties, need to be determined. In this paper, metallic vapours are focused on aluminium, iron and copper vapours in the consideration of industrial

[a] e-mail: liuyangrs@gmail.com

applications such as electrical apparatus and arc welding process. Numerous papers studied the thermodynamic or transport properties for pure CO_2 gas as well as mixtures of CO_2 and other gases; for example, CO_2–CF_3I mixtures [14], CO_2–PTFE mixtures [15], CO_2–SF_6 mixtures [16]. Besides, there are large quantities of papers about thermodynamic or transport properties of various gases containing metallic vapours; for instance, SF_6 mixed with copper vapour [17–20], air mixed with calcium, magnesium or iron vapours [21], air mixed with copper, iron, silver, or aluminium vapours [22–24], argon contaminated by iron, aluminium, chromium or manganese vapour [7], argon mixed with copper, iron or aluminium [25,26], nitrogen, helium and argon with consideration of copper, iron, aluminium or calcium vapours [27]. However, up to now, literature concerning thermodynamic and transport properties for CO_2 thermal plasma mixed by copper, iron or aluminium is extremely scarce in spite of the requirement of numerical modelling in industrial applications such as arc welding and electrical apparatus when CO_2 serves as a shielding or insulation gas.

Therefore, this paper is devoted to the calculation of thermodynamic and transport properties for CO_2 thermal plasma contaminated by metallic vapours: copper, iron and aluminium, and to the investigation of influences of metal on these thermophysical properties. Thermodynamic and transport properties of CO_2 plasma mixed with Al/Fe/Cu vapour of various concentrations are calculated assuming local thermodynamic equilibrium at atmosphere pressure with a temperature range of 2000–30,000 K since metals or their components may exist in the solid form under approximately 2000 K. In Section 2, the calculated results of equilibrium compositions and thermodynamic properties (mass density, specific enthalpy, specific heat) for CO_2–Al/Fe/Cu mixtures are exhibited in detail with a brief introduction of the calculation method. Moreover, the influence of metallic vapours (metal nature and concentrations) on these properties is investigated. In Section 3, transport coefficients of CO_2–Al/Fe/Cu mixtures are presented and the choice of potential models dealing with particle interactions is described. Lastly, conclusions are presented in Section 4.

2 Equilibrium composition and thermodynamic properties

To acquire thermodynamic properties depending significantly on plasma compositions, plasma compositions must be determined as a prerequisite. More specifically, assuming local thermodynamic equilibrium, the calculation of equilibrium compositions for CO_2–metal mixtures is conducted utilizing the Gibbs free energy minimization method as done in our previous work [15].

In the calculation of CO_2–metal mixtures 61 different species are taken into consideration: e^-, C, C_2, C_3, C_4, C_5, O, O_2, O_3, CO, CO_2, C_2O, C_3O_2, C^+, C^{2+}, C^{3+}, C^{2+}, O^+, O^{2+}, O^{3+}, O^{4+}, $O_2{}^+$, $O_3{}^+$, CO^+, $CO_2{}^+$, C^-, $C_2{}^-$, $C_3{}^-$, O^-, $O_2{}^-$, $O_3{}^-$, CO^- and $CO_2{}^-$ for CO_2 plasma, and in addition Cu, Cu_2, CuO, Cu^+, Cu^{2+}, Cu^{3+}, Cu^- for CO_2–Cu mixture, or Al, Al_2, AlO, Al_2O, AlO_2, Al_2O_2, Al^+, Al^{2+}, Al^{3+}, AlO^+, Al_2O^+, $Al_2O_2{}^+$, Al^-, AlO^-, $AlO_2{}^-$ for CO_2–Al mixture, or Fe, FeO, Fe^+, Fe^{2+}, Fe^{3+}, Fe^- for CO_2–Fe mixture. The basic parameters required to determine equilibrium composition are compiled from NIST–JANAF thermo-chemical tables [28]. Mass proportion is adopted to define mixing ratios of mixtures in this paper.

As an example, equilibrium compositions for CO_2 plasma contaminated with 1% Al and 10% Al (mass proportion) at atmosphere pressure with temperature up to 30,000 K are presented in Figures 1a and 1b, respectively. It can be found that the existence of Al element is mainly in form of Al_2O_2, AlO, Al_2O and AlO_2 at temperature below 3500 K, which can decrease the proportion of oxides and oxygen such that CO_2 and O_2 and can increase CO proportion marginally with hampering the reassembly of CO_2 at this temperature range. As temperature increases, dissociation and ionization reactions play a vital role in the determination of plasma compositions. It is notable that the existence of Al even in small concentration like 1% can change significantly the ion species at low temperature (approximate 6000 K). Specifically, within this temperature range, the predominant positive ion for CO_2–Al mixtures is Al^+ rather than C^+ for pure CO_2 gas. Besides, the reactions of ionization are stimulated to occur at lower temperature caused by the addition of Al. In fact, compared with neutral atoms like C and O (C 11.26 eV, O 13.62 eV), metal atoms (Al 5.986 eV, Fe 7.902 eV, Cu 7.726 eV) require a lower ionization energy, which can be furnished spontaneously at lower temperature. Furthermore, the mole fraction of electrons existing in CO_2–Al mixtures is enhanced dramatically at temperature range 4000–9000 K with the addition of Al but is altered minimally at temperature above around 13,400 K. Similar behaviour can also be observed for CO_2–Cu mixtures and CO_2–Fe.

To acquire thermodynamic properties, equilibrium compositions are utilized via thermodynamic equations, which is demonstrated in our previous work [19]. Thermodynamic properties, such as mass density, specific enthalpy and specific heat at constant pressure, are usually required by numerical simulation for diverse applications. Figure 2 exhibits the variations of mass density for pure CO_2 and pure metallic vapours including Al, Fe and Cu at atmosphere pressure. Taken together, these curves for mass density have a tendency to decrease with temperature, which is accompanied by slope fluctuation representing dissociation and ionization processes. Specifically, mass densities for Cu and Fe have quite similar variations. Mass density for Al is lower than that for other metallic vapours but is higher than that for CO_2 at temperature above 3500 K, which can be attributed to the different atomic masses (Al 26.9 $g\,mol^{-1}$, Fe 55.8 $g\,mol^{-1}$, Cu 63.5 $g\,mol^{-1}$). It is interesting to find that the mass density for pure Al at temperature below 3500 K is lower than that for pure CO_2. Although its atomic mass is higher than that of Al, CO_2 dissociates strongly into CO and O and is not a dominant species at this temperature interval.

Variations of specific enthalpy at atmosphere pressure for pure CO_2, pure metals (Al, Fe, Cu) and CO_2 mixed

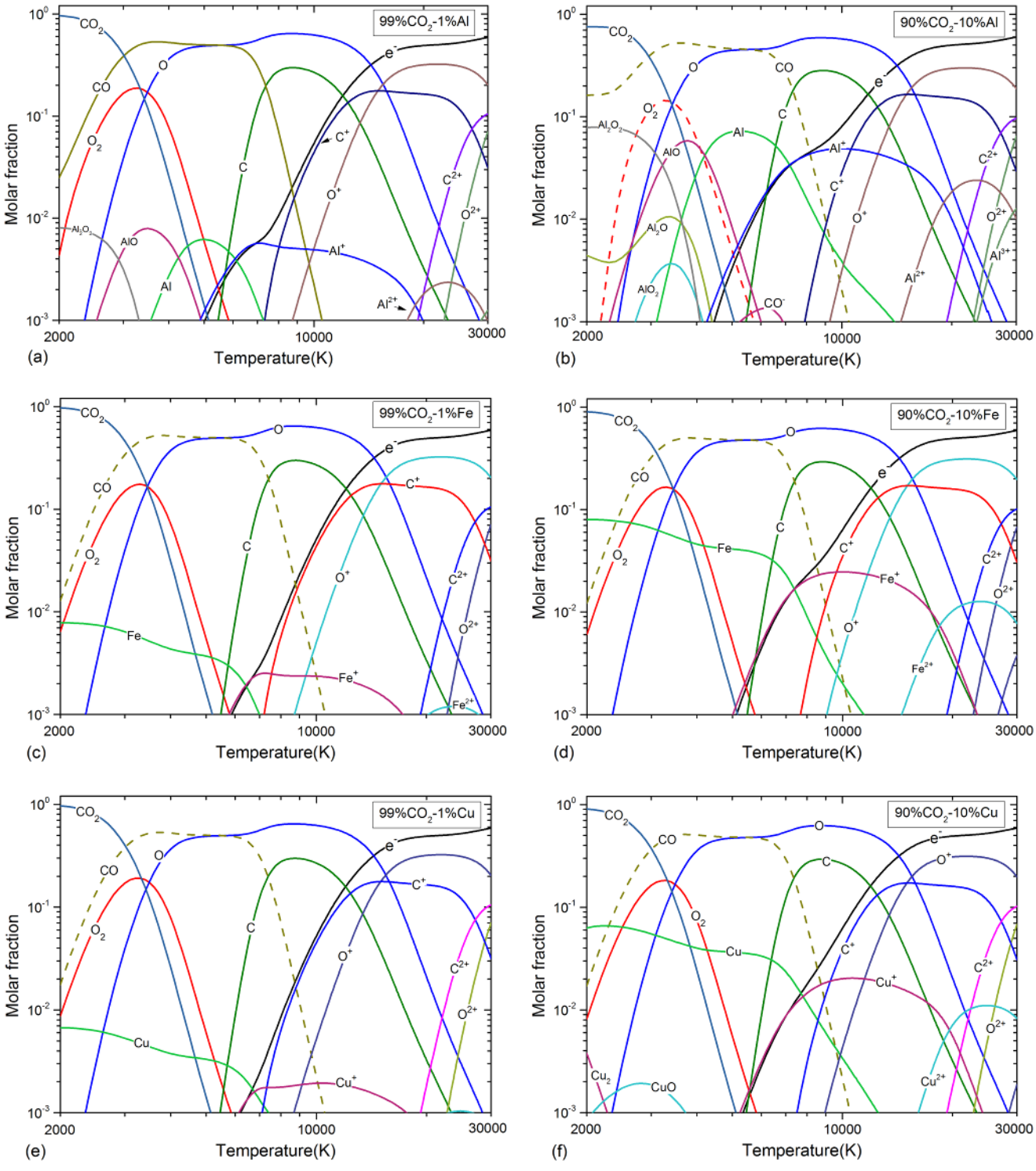

Fig. 1. Equilibrium compositions for (a) 99% CO_2–1% Al mixtures, (b) 90% CO_2–10% Al mixtures, (c) 99% CO_2–1% Fe mixtures, (d) 90% CO_2–10% Fe mixtures, (e) 99% CO_2–1% Cu mixtures and (f) 90% CO_2–10% Cu mixtures at 1 bar.

with 10% metal are presented in Figure 3. It can be observed that, among metals, the enthalpy of Al is much higher than that of other metals. Moreover, the enthalpy of Fe is close to that of Cu, which results in rather similar effects on the enthalpy of CO_2. Compared to CO_2, however, all kinds of metal considered in this paper present a much lower enthalpy at temperature above 7300 K, suggesting that nonmetallic particles need more energy to dissociate and ionize than metallic particles. Taken together, metals of small proportion, especially Al, have only a noticeable effect on the specific enthalpy for CO_2.

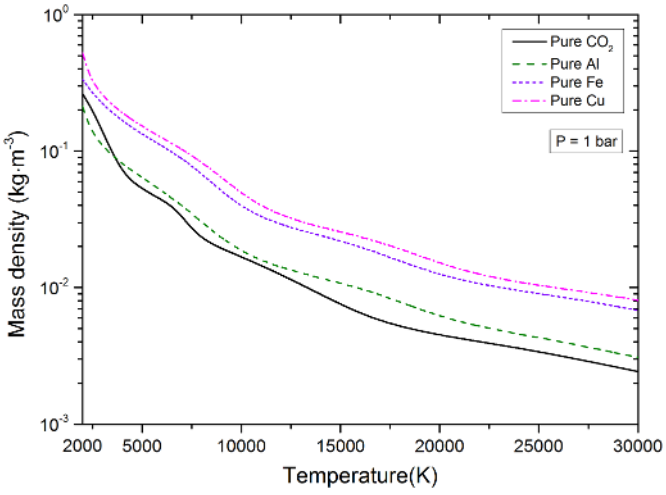

Fig. 2. Mass density for CO_2, Al, Fe and Cu at 1 bar.

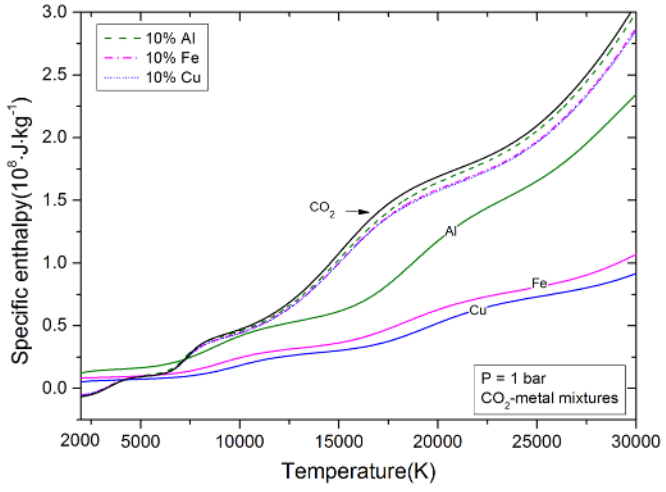

Fig. 3. Specific enthalpy of CO_2, metallic vapours (Al, Fe, Cu) and 90% CO_2–10% metal mixtures at 1 bar.

Figure 4a illustrates the evolutions of specific heat for pure CO_2, pure metals and CO_2 mixed with 10% metallic vapour at atmosphere pressure. The specific heat, the derivative of enthalpy with respect to temperature at constant pressure, is evidenced by the enthalpy shown in Figure 3, and peaks of curves are correlated to reactions of dissociation and ionization. For pure metal vapours, the peaks at temperatures above 5000 K represent the successive ionizations of metal atom. At around 2000 K, however, the enthalpy for Al and Cu reveals peaks which are not observed for Fe. Assuming all components are gaseous species, the compositions for pure Al, taken as an example, are exhibited in Figure 4b to investigate this phenomenon and it was found that the peak at approximately 2000 K could result from this dissociation reaction $Al_2 \rightarrow Al$. Besides, it can be observed that the addition of metals, in general, can decline the specific heat for CO_2 due partially to the enhanced mass density, which is not so marked with a metal concentration of 10%. Moreover, copper and iron vapours indicate quite similar effects on specific heat for CO_2.

The influence of gas pressure on thermodynamic properties are investigated as follows. CO_2–metal mixtures exhibit similar properties and are strongly dominated by properties of CO_2 when metallic concentration is small. Thus, we take 80% CO_2–20% Cu mixture as an example to illustrate the effect of gas pressure on thermodynamic properties, as shown in Figure 5.

Increasing pressure delays the dissociation and ionization reactions and compresses the gas mixtures. Therefore, heavier molecules can stay longer and the number density is enhanced, leading the increase of mass density. The evolution of specific enthalpy can be attributed to the chemical reactions and change of mass density when increasing pressure. For specific heat, peaks are shifted to higher temperatures with amplitudes attenuated, which is mainly due to the delayed chemical reactions.

3 Determination of transport coefficients

Based on the classical Chapman–Enskog method detailed by Hirschfelder et al. [29], transport properties (viscosity, electrical and thermal conductivity) are determined approximately by utilizing selected-order approximations of solutions to the Boltzmann equation. The formula established by Devoto [30] through the third approximation for partially ionized gas in LTE is utilized in our work to calculate electrical conductivity neglecting the contribution of ions. The viscosity, resulting from a velocity gradient and representing momentum transport process, is often computed by a first-order approximation of the Chapman–Enskog method with an assumptive independence of viscosity on electron properties. This is due to the rather high mass ratio of heavy particle and electron on physical grounds [31]. Thermal conductivity κ contains three parts [32]: the first one, internal thermal conductivity, which corresponds to internal energy transport, can be calculated from a second-order approximation of Chapman–Enskog method; second one, reaction thermal conductivity, which represents chemical reaction processes like dissociations, recombinations and ionizations, is computed based on Butler and Brokaw method [33] extending to ionized mixtures; third one, translational thermal conductivity, resulting from translation of electrons and heavy particles, is developed by approximating to a second- and third-order of Chapman–Enskog method, respectively [30]. For the sake of our calculation, comparisons with the literature results are essential, which have been performed in our previous paper [15,34] for pure CO_2 and pure copper and have achieved a good agreement.

Previous studies have demonstrated that collision integrals play a critical role in the determination of transport coefficients. Thus, the computation of collision integrals is most essential and difficult to deal with all binary collisions, since collision integrals could affect transport coefficients significantly.

3.1 Collision integrals

To acquire collision integrals, four categories of interactions between different species are considered, which are as follows.

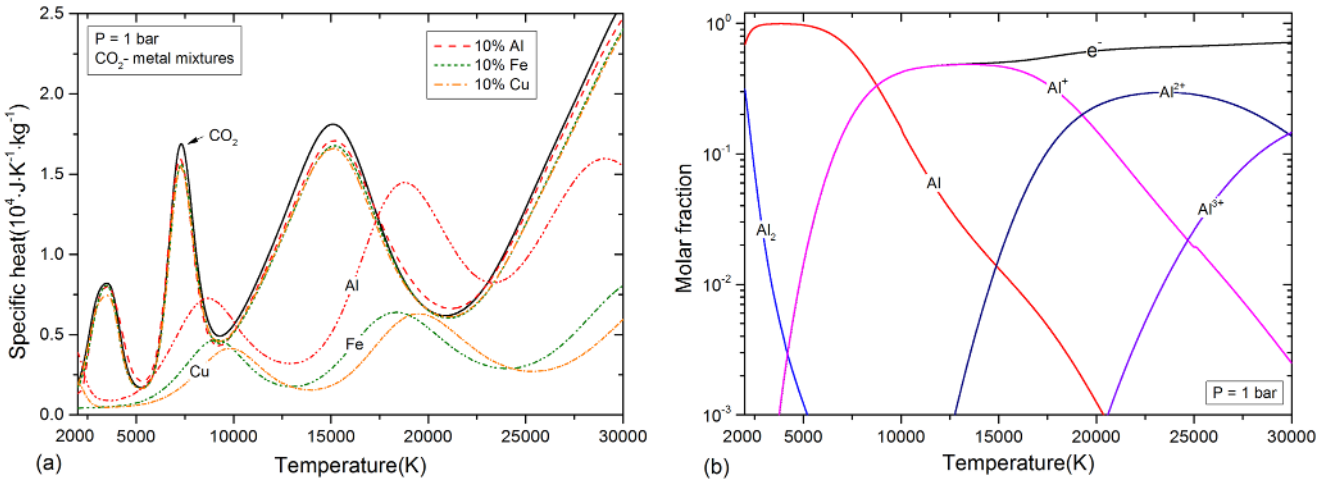

Fig. 4. (a) Specific heat of various 90% CO_2–10% metal mixtures at 1 bar. (b) Equilibrium composition for pure Al at 1 bar.

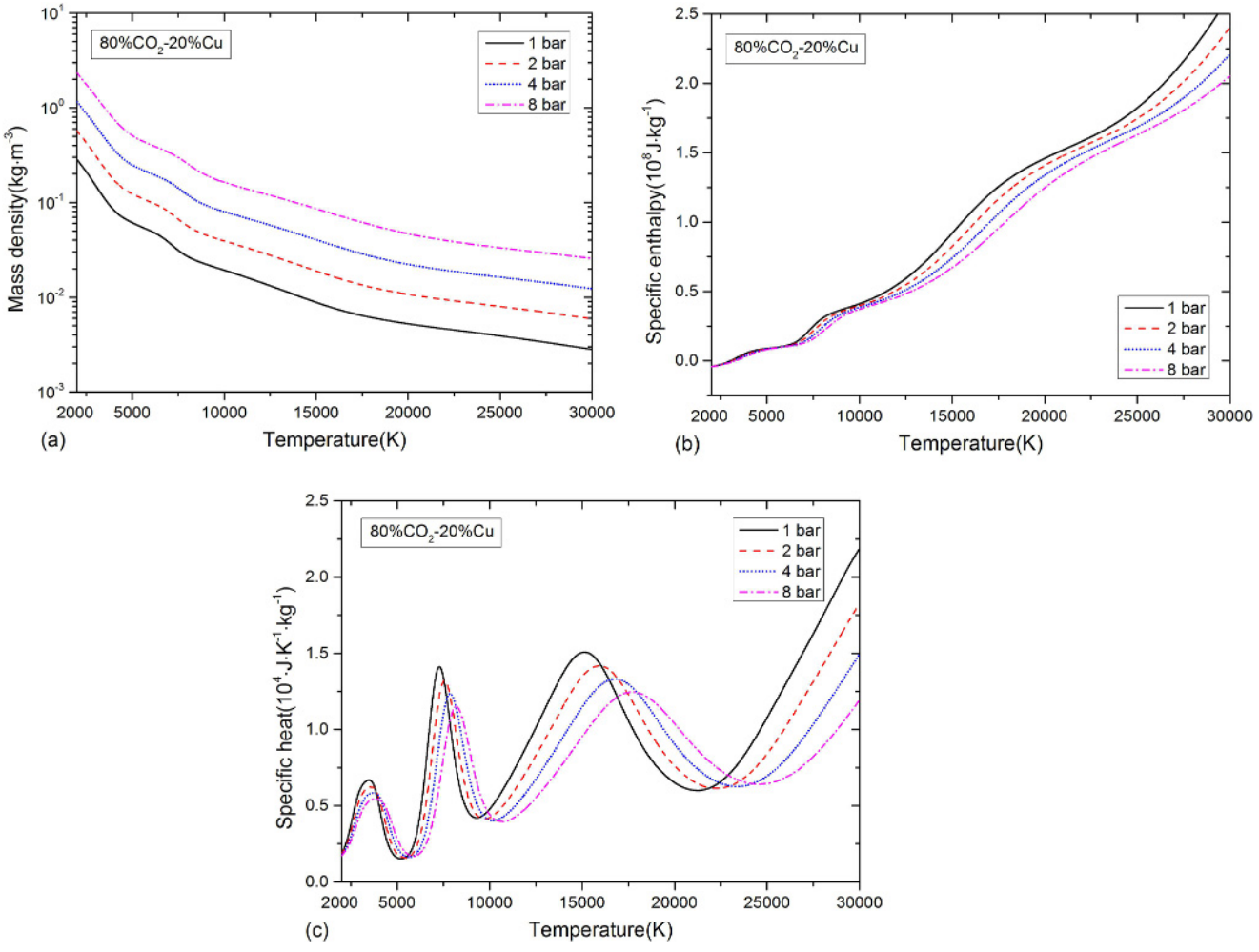

Fig. 5. Thermodynamic properties of 80% CO_2–20% Cu mixtures for different pressure. (a) Mass density, (b) specific enthalpy, (c) specific heat.

Table 1. Potentials or method adopted to calculate electron–neutral collision integrals.

	Method	Reference
e-C	Integration of cross section	[15]
e-O	Integration of cross section	[15]
e-C_2	Integration of cross section	[15]
e-O_2	Integration of cross section	[15]
e-CO	Integration of cross section	[15]
e-CO_2	Integration of cross section	[15]
e-C_2O	Integration of cross section	[15]
e-Al	Integration of cross section	[25]
e-Al_2	Estimation from e-Al	[26,39]
e-AlO	Polarization potential	[24]
e-AlO_2	Polarization potential	[24]
e-Al_2O	Polarization potential	[24]
e-Al_2O_2	Polarization potential	[24]
e-Fe	Integration of cross section	[25]
e-FeO	Polarization potential	[22]
e-Cu	Integration of cross section	[34]
e-Cu_2	Polarization potential	[22]
e-CuO	Polarization potential	[22]

Table 2. Potentials or data used to calculate the collision integrals of ion–neutral interactions.

	C	O	O_2	CO	Cu	Fe
C^+	[41]	Len	Len	Len	Len	Len
O^+	Len	[42]	Len	Len	Len	Len
$O_2{}^+$	Len	Len	[43]	Len	Len	Len
CO^+	Len	Len	Len	[43]	Len	Len
$O_3{}^+$	Pol	Pol	Pol	Pol	Pol	Pol
$C_3{}^-$	Pol	Pol	Pol	Pol	Pol	Pol
Cu^+	Len	Len	Len	Len	[44]	—
Cu^{2+}	Pol	Pol	Pol	Pol	Pol	—
Cu^{3+}	Pol	Pol	Pol	Pol	Pol	—
Fe^+	Len	Len	Len	Len	—	[22]
Al^{2+}	Pol	Pol	Pol	Pol	—	—
Al^{3+}	Pol	Pol	Pol	Pol	—	—
Al_2O^+	Pol	Pol	Pol	Pol	—	—
$Al_2O_2{}^+$	Pol	Pol	Pol	Pol	—	—
Al^-	Pol	Pol	Pol	Pol	—	—

Notes. Len – Lennard-Jones like phenomenological potential; Pol – polarizability potential; interactions that are not mentioned in Table 2 are all described by Lennard-Jones like phenomenological potential.

For neutral–neutral interactions, as an improvement of other approaches, Lennard-Jones like phenomenological potential, proposed by Laricchiuta [35] and validated by Capitelli [36], was adopted to describe neutral–neutral interactions calculating corresponding collision integrals with the similar consideration demonstrated in our previous work [19,37]. Polarizability of neutral species, as an essential parameter in the determination of this mentioned potential, is compiled from NIST Computational Chemistry Comparison and Benchmark Database [38] except species containing Al and Fe element from literature [22,24].

For electron–neutral interactions, collision integrals of e-C, e-O, e-C_2, e-O_2, e-CO, e-CO_2 and e-C_2O are obtained by conducting numerical integrations of the transport cross section compiled in literature [15]. Transport cross sections for e-Al, e-Fe and e-Cu are compiled from [25]. The collision integrals for e-Al_2 are estimated from e-Al following the relation proposed by Andre et al. [39]. Additionally, for interactions between electron and species containing AlO, AlO_2, Al_2O, Al_2O_2, FeO, Cu_2 and CuO, the polarization potential is applied following the work of Cressault et al. [22,24]. The methods used to deal with electron–neutral interactions are reported in Table 1.

For ion–neutral interactions, elastic collision process and resonant charge exchange process are considered [17,40]. For the interactions dominated by resonant charge exchange process, CO–CO^+, Cu–Cu^+, O–O^+, C–C^+ and O_2–$O_2{}^+$ are taken into consideration in this work, for which the corresponding parameter A and B utilized to evaluate transport cross section are detailed in our previous work [34]. However, the collisions for the other ion–neutral interactions are considered as elastic. More specifically, Lennard-Jones like phenomenological potential, for elastic collision process, was preferred to deal with a collision between charged and neutral particles, while the polarization potential was adopted for charged particles without available polarizability values. Potentials or data used to treat ion–neutral interactions are reported in Table 2.

Interactions between charged species are usually described by the screened Coulomb potential [45] using the Debye radius as the screening distance. The definition of the Debye radius arouses some debate on the question of whether only electron or both electron and ion contributions should be considered to calculate Debye length. In this work, only electrons were considered to compute the Debye length according to the work of Murphy [46,47] and Devoto [48].

3.2 Transport properties

3.2.1 Electrical conductivity

As shown in Figures 6a and 6b, the effect of metallic vapours (Al, Fe, Cu) on the evolution of electrical conductivity for CO_2 at atmospheric pressure is investigated. Obviously, the electrical conductivity for CO_2 is enhanced dramatically with the addition of minimal metallic vapours at temperature below 8500 K. This behaviour can be attributed to the increase of electron number density, as shown in Figure 6c, resulting from the added metal with lower ionization energy (Al 5.986 eV, Cu 7.726 eV, Fe 7.902 eV) than other neutral species (C 11.2603 eV, O 13.6181 eV). Such mechanism is evidenced by that Al has the largest electrical conductivity among pure gases at temperatures below 10,000 K because ionization of Al atoms occurs easier than other atoms and, consequently, Al modifies the electrical conductivity for CO_2 more significantly than other metals. However, at high temperature, the addition of metals indicates a reverse tendency towards the electrical conductivity for CO_2. The reason for this phenomenon may

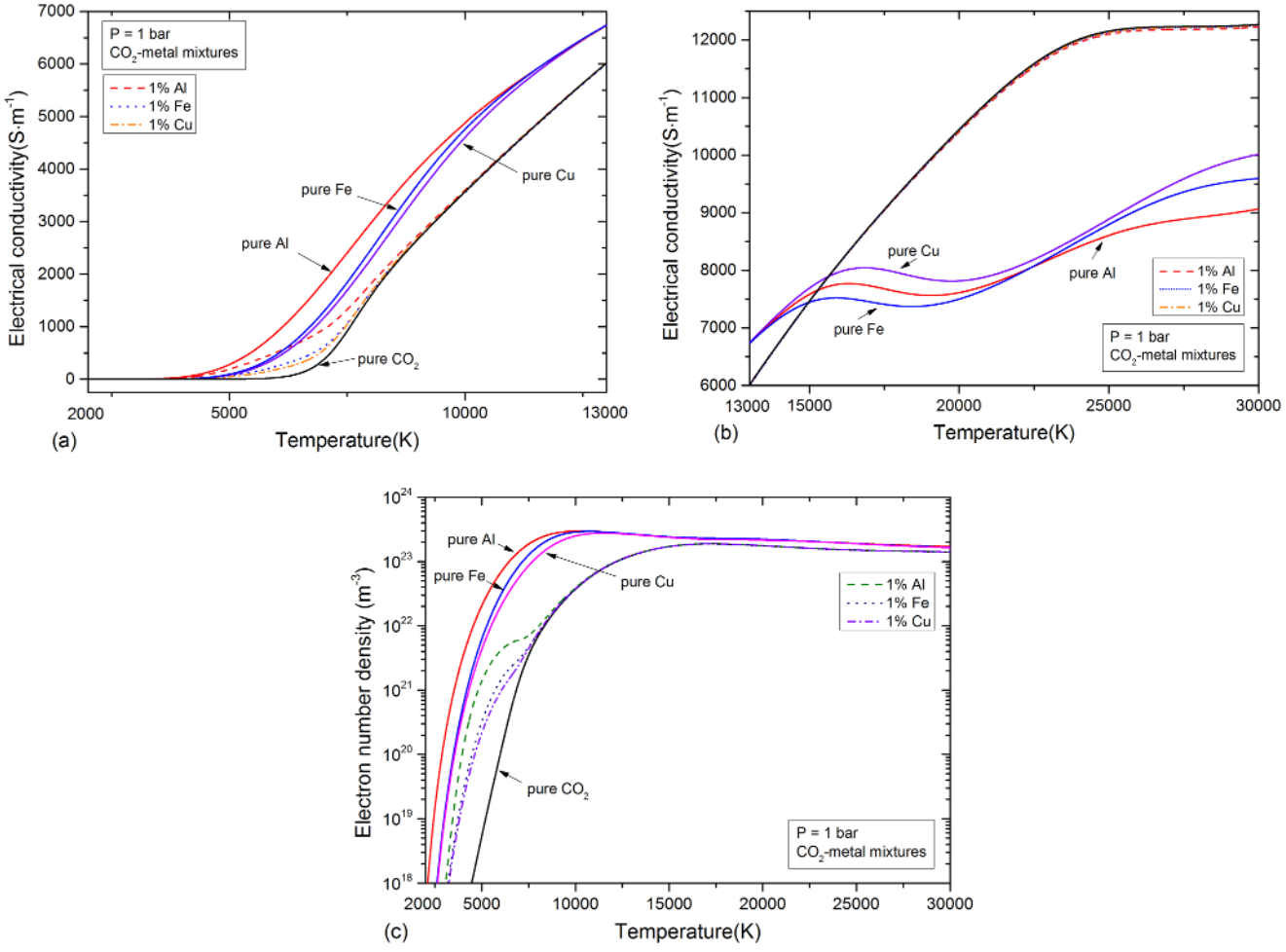

Fig. 6. (a) Electrical conductivity of 2000–13,000 K. (b) Electrical conductivity of 13,000–30,000 K. (c) Electrical number density for pure CO_2, pure metals (Al, Fe, Cu) and 99% CO_2–1% metal mixtures at 1 bar.

be the serval opposite processes: the raised electron number density and the essential charge–charge interactions. Although ionizations produce more electrons tending to increase electrical conductivity, the generated multiple ionized particles result in larger collision integrals due to the domination of Coulomb potential, which hinders the increase of electrical conductivity. In addition, Fe and Cu present quite close evolutions of electrical conductivity and indicate a similar influence on electrical conductivity of CO_2 under same mixing ratio.

3.2.2 Viscosity

Figure 7 illustrates the influence of metals on the viscosity at atmospheric pressure with temperature up to 30,000 K. It can be observed that the addition of metals (Al, Fe, Cu) to CO_2 leads to a decline of viscosity, especially at temperature interval 3000–14,000 K. It is classically known that the peak of viscosity represents a transform of a gas governed by neutral particles into a plasma dominated by ionized particles. As Cressault et al. concluded [24], the amplitude and position of the peak for viscosity is related to the masses and ionization energies as well as collision integrals $\overline{\Omega}^{(1-1)}_{X-X}$ and $\overline{\Omega}^{(2-2)}_{X-X}$ of species present in the plasma. Compared with other species, aluminium has a lowest ionization energy and mass and therefore the viscosity exhibits a smallest peak. Before reaching maximum, viscosity shows a quasi-linear relationship with temperature, which is strongly determined by properties of species present in the plasma. Then, after reaching the maximum, charged particles become predominant and the viscosity descends owing to the larger Coulomb collision integrals. Besides, Al modifies the viscosity for CO_2 more dramatically than Fe or Cu. In addition, the effect of Fe or Cu on the viscosity for CO_2 is rather similar and negligible at the concentration of 10%. Metals present peaks at lower temperatures, which are quite close than CO_2 owing to the lower ionization potential, and consequently ionization degree.

3.2.3 Thermal conductivity

Figure 8 investigates the effect of metals on the total thermal conductivity of CO_2 plasma. It can be observed that generally the addition of metals to CO_2 will reduce the thermal conductivity. The reason for the decline of

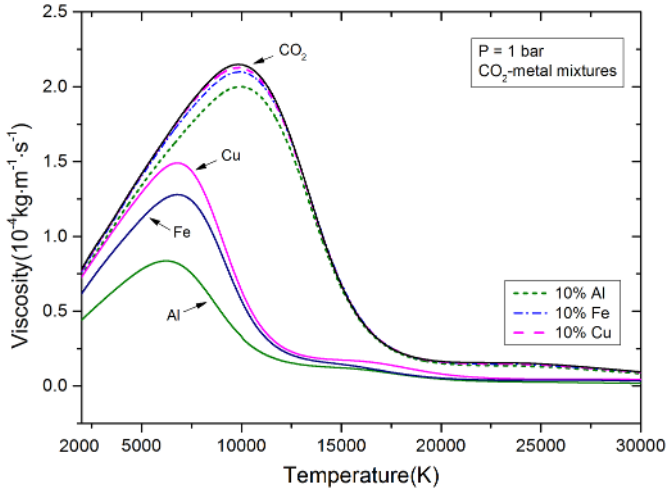

Fig. 7. Viscosity for pure CO_2, pure metals (Al, Fe, Cu) and 10% CO_2–10% metal mixtures at 1 bar.

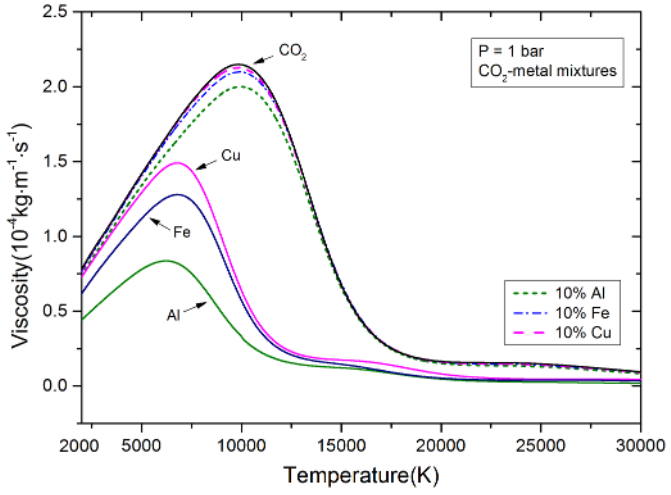

Fig. 8. Thermal conductivity of CO_2, metallic vapours (Al, Fe, Cu), 50% CO_2–50% metal mixtures and 90% CO_2–10% metal mixtures at 1 bar.

thermal conductivity with adding metal at low temperature can be explained by a relative decrease of CO_2 and the less energy required by the ionization of metal atoms due to the dominance of reaction thermal conductivity in this temperature interval. At high temperature, charged particles, as majority species, lead to larger collision integrals, which cause a decline of thermal conductivity. The peaks of thermal conductivity represent different reactions that are similar to those for specific heat. In addition, the existence of metals with a concentration of 10% has a rather limited influence on the thermal conductivity in CO_2-metal mixtures. Besides, an interesting phenomena is observed: the first peak of 50% CO_2–50% Al mixture presents a larger amplitude, which occurs at higher temperature than the first peaks of 50% CO_2–50% Fe mixture and 50% CO_2–50% Cu mixture. The reason can be attributed to the dissociation reactions considered in the calculation.

The influence of gas pressure on transport are investigated as shown in Figure 9, taking 80% CO_2–20% Cu as an example. For electrical conductivity, at low temperature increasing pressure declines the electrical conductivity, whereas an opposite effect is observed at high temperature. Obviously, increasing pressure will lead to continuous growth of species number density, including electron number density for a given temperature. At high temperatures, electron and ions are dominant species and electron number density increases with pressure, consequently leading to growth of electrical conductivity. However, at low temperature, electron–neutral interactions are dominant. Ionization processes are hindered by increasing pressure and electron number density cannot grow rapidly with pressure as other species. Besides, collision integrals of electron–neutral interactions are much lower than those of ion–ion interactions.

Viscosity of CO_2–Cu mixture shows almost independence on pressure when temperature is below 7000 K since viscosity is strongly related to temperature in this temperature interval. Above 7000 K, viscosity shows an upward tendency with pressure and simultaneously the peak is shifted to higher temperature with increasing pressure. These phenomena can be attributed to the hindered ionization process, resulting in a drop of ionization degree and consequently a declined contribution to integrals of Coulomb collisions.

As for thermal conductivity, increasing pressure results in attenuated peaks with a shift to higher temperatures below 12,000 K and leads to an enhancement of thermal conductivity above 12,000 K. These phenomena can be mainly attributed to suppression of dissociation and ionization with increasing pressure.

Mixing rules for transport coefficients have been widely studied in literature for benefits of simplicity of calculations and convenient access of pure gas properties, which might be essential in some industrial applications. The best well-known mixing rules might be the formula proposed by Wilke [49] and improved by Vanderslice et al. [50], which might be less dependable for some plasmas [51–53].

Some of the results obtained through the molar/mass fraction averages mixing rules and Wilke's approximation are shown in Figure 10 to compare these mixing rules with respect to electrical conductivity, viscosity and thermal conductivity for 80% CO_2–20% Cu mixtures and 80% CO_2–20% Fe mixtures.

As for electrical conductivity, the approximation of linear interpolation (mass, molar) is less satisfactory for temperature below 10,000 K for either CO_2–Cu or CO_2–Fe mixtures. This mixing rule underestimates the increase of electrical conductivity due to the metal vapour addition and predicts in a lower electrical conductivity than the exact values. At high temperature, linear interpolation is more reliable.

As for viscosity, these mixing rules exhibit quite close variations for both CO_2–Cu mixtures and CO_2–Fe mixtures. The amplitude of peaks predicted by mixing rule is lower than that of exact solution and the peaks predicted occur at lower temperature. Besides, Wilke's approximation does not present better results

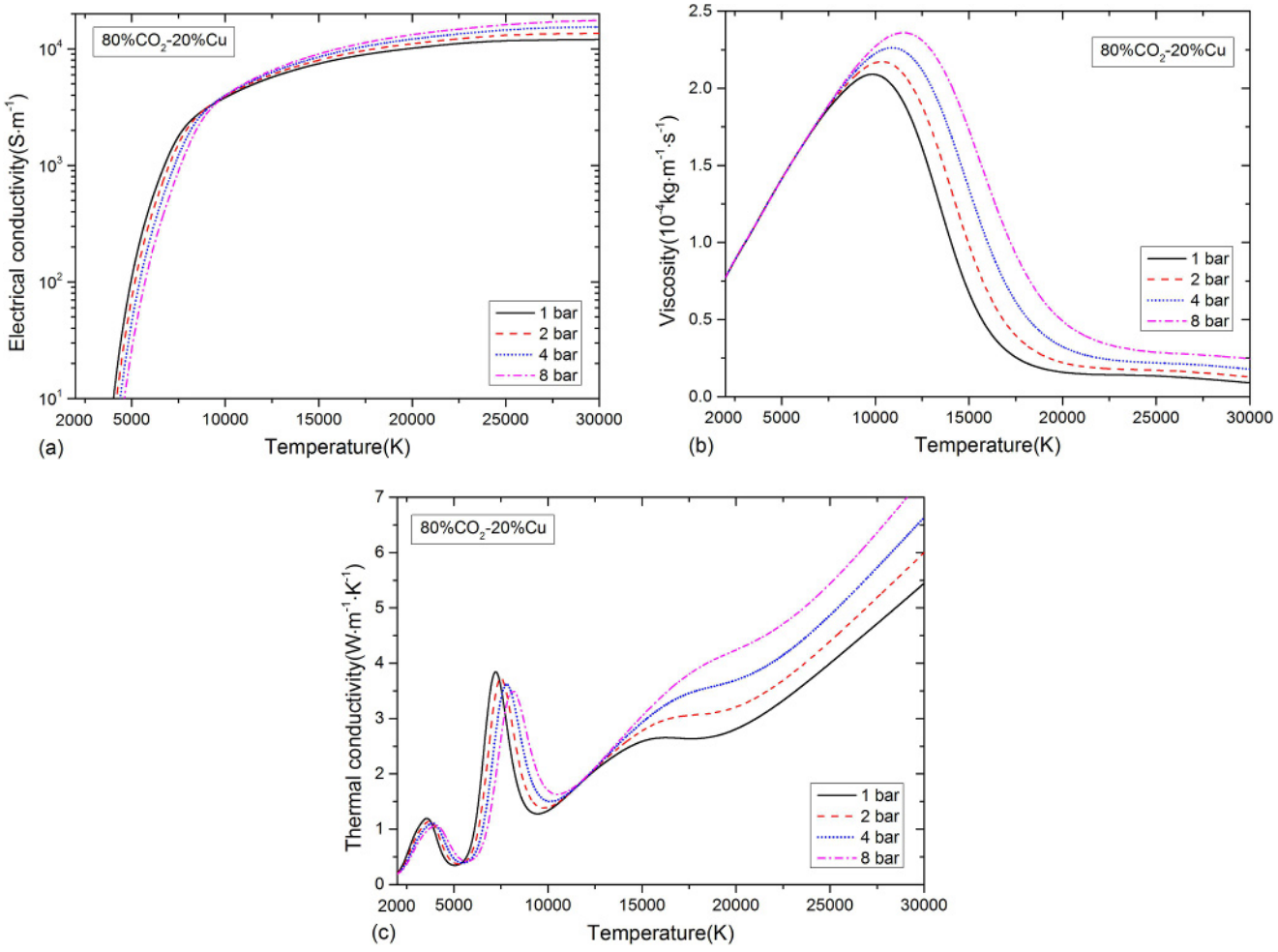

Fig. 9. Transport coefficients of 80% CO_2–20% Cu mixtures for different pressure. (a) Electrical conductivity, (b) viscosity, (c) thermal conductivity.

than molar/mass average mixing rules except for CO_2–Cu mixtures.

As for thermal conductivity, the method of Wike's approximation is only applicable for translation thermal conductivity. In fact, however, besides translation thermal conductivity, reaction thermal conductivity is also one of vital component of thermal conductivity, which is strongly related with peaks of thermal conductivity. Thus, it is less satisfactory to adopt Wilke's approximation to describe the variation near the peaks, as shown in Figures 10e and 10f. The method of Wilke's approximation is not better than molar/mass average mixing rules. Furthermore, because the thermal conductivity of CO_2 is much higher than that of copper or iron vapour, the thermal conductivity of mixtures is governed by CO_2. Moreover, it can be expected that the mixing rules would present more reliable results when the concentration of metal vapour is rather low.

These properties for CO_2–metal mixtures are essential parameters in arc modelling, especially for CO_2 circuit breakers taking account of the electrode vaporization.

For circuit breakers, it is well known that the thermal interruption capability depends strongly on the turbulent exchange that plays a vital role in the energy transfer between the arc and surrounding gas [54,55]. Turbulent effect leads to an enhanced thermal conductivity, and energy transfer can be represented by the term of ρCp. Liu et al. found that the excellent interruption capability of a gas media requires highest possible values of ρCp at temperature interval where electrical conduction does not occur and at lowest possible values of ρCp above this temperature (around 4500 K, Fig. 6a) [56]. Consequently, these characteristics result in a small size arc with high axial heat conduction and high radial heat conduction in edge regions. For instance, the variation of ρCp of SF_6 presents no peaks above 4500 K while two large peaks below this temperature where electrical conduction does not occur, as shown in Figure 11. Thus, the arc quenching capability is superior to other gases such as CO_2. For CO_2 mixing with 1% Cu, 10% Cu and 30% Cu, the variation of ρCp exhibits two peaks at around 3000 K and 7300 K. The first peak, which happens at temperature before the beginning of electrical conduction, will enhance the radial heat conduction. However, the second peak at temperature which electrical conductivity cannot be neglected is undesirable and could result in a broad arc core with slow

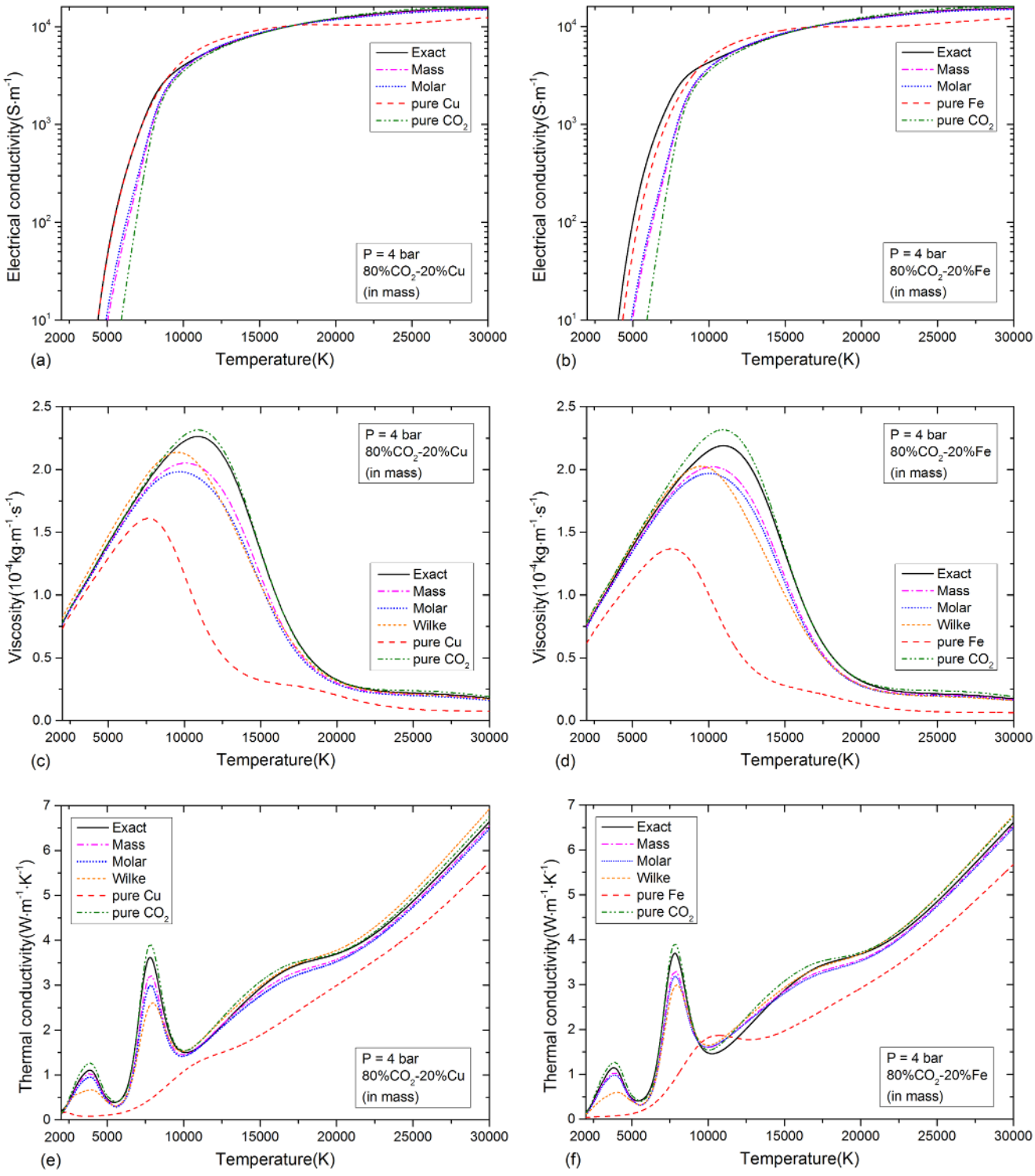

Fig. 10. Comparison of approximation rules with the exact values of electrical conductivity, viscosity and thermal conductivity for 80% CO_2–20% Cu mixtures and 80% CO_2–20% Fe mixtures ('Mass' and 'Molar' for mass molar average mixing rules, respectively; 'Wilke' for Wilke's approximation).

temperature decay. In addition, the presence of copper decreases the amplitude of the peak at around 3000 K but barely modifies the other peak at around 7300 K. These phenomena will reduce the radial heat conduction below temperature where electrical conductivity is negligible and lead to a broad arc core, which means weaker thermal arc interruption capability. Besides, copper vapour makes the electrical conduction occur at lower temperature due to the smaller ionization energy of Cu, as shown in Figure 6. This process is adverse to the arc

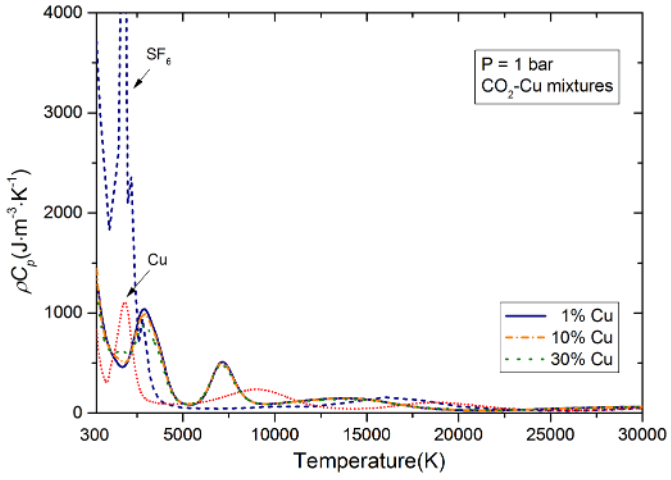

Fig. 11. ρCp of SF_6[17], Cu and CO_2 mixing with 1%, 10% and 30% Cu.

extinction that is accomplished by eliminating electrical conductivity.

Based on this discussion, it can be found that the interruption capability of CO_2 is lower than that of SF_6 and the copper vapour from electrode erosion further hinders arc extinction. Moreover, arc modelling is indispensable to obtain an overall evaluation of the arc extinction in CO_2 circuit breakers with the consideration of copper vapour.

4 Conclusion

In this study, using Gibbs free energy minimum method and classical Chapman–Enskog theory, we studied the effects of various metals, namely, Al, Fe and Cu, on the fundamental properties of CO_2 plasma at temperatures of 2000–30,000 K. Comparison with the limited results of metals published by other researchers are conducted to validate our calculation.

Because of low ionization energy (Al, Fe and Cu), metals, even if a rather small concentration like 1%, can change significantly the charged species at low temperature and result in more electrons at lower temperature, consequently enhancing the electron number density of CO_2–metal mixtures.

As a result, the electrical conductivity, especially at low temperature, is significantly enhanced by the existence of metals. More specifically, Al increases electrical conductivity more dramatically than other metals (Fe, Cu). Moreover, Fe and Cu reveal a quite close electrical conductivity and present a similar effect on electrical conductivity of CO_2 under the same mixing ratio.

However, for viscosity and thermal conductivity of CO_2, the attenuating effects of metals, particular Fe and Cu, are quite marginal with a concentration of 10%. Al and Fe present a similar thermal conductivity whose peaks are slightly higher than that of Cu and the peak positions for these metals are near.

Besides, metals indicate a slightly attenuating influence on the enthalpy and specific heat for CO_2 with a small concentration of 10%. Fe and Cu present similar revolutions for these thermodynamic properties.

Gas pressure modifies thermophysical properties of CO_2–metal mixtures significantly. Electrical conductivity is deduced by increasing pressure at low temperature, whereas an opposite influence is at high temperature. Above 7000 K, viscosity is enhanced and peaks are shifted to higher temperature. Thermal conductivity is attenuated below 12,000 K and enhanced above this temperature with peaks shifted to higher temperature. The reason can be attributed to the suppression of chemical reactions and modification of species number density.

This work was supported by National Natural Science Foundation of China (No. 51521065) and Pinggao Group Co. Ltd. (No. JSKF(2015)1065).

Author contribution statement

Aijun Yang proposed the research topic. Xiaohua Wang and Mingzhe Rong offered valuable suggestions during the research and supported the study. Linlin Zhong provided theoretical guidance of calculation method. Yang Liu analysed the data and wrote the paper. Junhui Wu provided valuable discussion in this work.

References

1. M.I. Boulos, P. Fauchais, E. Pfender, *Thermal plasmas: fundamentals and applications* (Springer Science +Business Media, 2013)
2. L. Pershin, L. Chen, J. Mostaghimi, J. Therm. Spray Tech. **17**, 608 (2008)
3. M. Tanaka, J.J. Lowke, J. Phys. D: Appl. Phys. **40**, R1 (2007)
4. B. Swierczynski, J.J. Gonzalez, P. Teulet, P. Freton, A. Gleizes, J. Phys. D: Appl. Phys. **37**, 595 (2004)
5. T. Uchii, A. Majima, T. Koshizuka, H. Kawano, in *Proceedings of the 18th International Conference on Gas Discharges and Their Applications (GD2010)* (2010), p. 78
6. LTA 72D1 CO_2 high voltage circuit breaker. http://www.ABB.com/highvoltage
7. A.B. Murphy, J. Phys. D: Appl. Phys. **43**, 434001 (2010)
8. J.J. Gonzalez, M. Bouaziz, M. Razafinimanana, A. Gleizes, Plasma Sources Sci. Technol. **6**, 20 (1997)
9. M. Schnick, U. Füssel, M. Hertel, A. Spille-Kohoff, A.B. Murphy, J. Phys. D: Appl. Phys. **43**, 022001 (2010)
10. J.L. Zhang, J.D. Yan, M.T. Fang, IEEE Trans. Plasma Sci. **32**, 1352 (2004)
11. V. Liau, B. Lee, K. Song, K. Park, J. Phys. D: Appl. Phys. **39**, 2114 (2006)
12. J.C. Lee, Y.J. Kim, Vacuum **81**, 875 (2007)
13. A. Gleizes, J.J. Gonzalez, P. Freton, J. Phys. D: Appl. Phys. **38**, R153 (2005)
14. Y. Yokomizu, R. Ochiai, T. Matsumura, J. Phys. D: Appl. Phys. **42**, 215204 (2009)
15. A. Yang, Y. Liu, B. Sun, X. Wang, Y. Cressault, L. Zhong, M. Rong, Y. Wu, C. Niu, J. Phys. D: Appl. Phys. **48**, 495202 (2015)

16. W. Wang, W. Wang, M. Rong, Y. Wu, J.D. Yan, J. Phys. D: Appl. Phys. **47**, 255201 (2014)
17. B. Chervy, A. Gleizes, M. Razafinimanana, J. Phys. D: Appl. Phys. **27**, 1193 (1994)
18. K.C. Paul, T. Sakuta, T. Takashima, M. Ishikawa, J. Phys. D: Appl. Phys. **30**, 103 (1997)
19. M. Rong, L. Zhong, Y. Cressault, A. Gleizes, X. Wang, F. Chen, H. Zheng, J. Phys. D: Appl. Phys. **47**, 495202 (2014)
20. Y. Wu, Z. Chen, F. Yang, Y. Cressault, A.B. Murphy, A. Guo, Z. Liu, M. Rong, H. Sun, J. Phys. D: Appl. Phys. **48**, 415205 (2015)
21. Y. Tanaka, Y. Yokomizu, M. Kato, T. Matsumura, K. Shimizu, S. Takayama, T. Okada, in *The 4th International Thermal Plasma Processes Conference, Athens, Greece* (1996), p. 15
22. Y. Cressault, R. Hannachi, P. Teulet, A. Gleizes, J.P. Gonnet, J.Y. Battandier, Plasma Sources Sci. Technol. **17**, 035016 (2008)
23. Y. Cressault, A. Gleizes, J. Phys. D: Appl. Phys. **43**, 434006 (2010)
24. Y. Cressault, A. Gleizes, G. Riquel, J. Phys. D: Appl. Phys. **45**, 265202 (2012)
25. Y. Cressault, A. Gleizes, J. Phys. D: Appl. Phys. **46**, 415206 (2013)
26. Y. Cressault, A.B. Murphy, P. Teulet, A. Gleizes, M. Schnick, J. Phys. D: Appl. Phys. **46**, 415207 (2013)
27. T. Hoffmann, G. Baldea, U. Riedel, Proc. Combust. Inst. **32**, 3207 (2009)
28. M. Chase, J.C. Davies, *NIST-JANAF thermochemical tables*, 4th edn. (American Institute of Physics for the National Institute of Standards and Technology, New York, 1998)
29. J.O. Hirschfelder, C.F. Curtiss, R.B. Bird, *Molecular theory of gases and liquids*, 2nd edn. (John Wiley & Sons, Inc., New York, 1964)
30. R.S. Devoto, Phys. Fluids **10**, 2105 (1967)
31. R.S. Devoto, Phys. Fluids **10**, 2704 (1967)
32. J. Vanderslice, S. Weissman, E. Mason, R. Fallon, Phys. Fluids **5**, 155 (1962)
33. J.N. Butler, R.S. Brokaw, J. Chem. Phys. **26**, 1636 (1957)
34. A. Yang, Y. Liu, L. Zhong, X. Wang, C. Niu, M. Rong, G. Han, Y. Zhang, Y. Lu, Y. Wu, Plasma Chem. Plasma Process. **36**, 1141 (2016)
35. A. Laricchiuta, G. Colonna, D. Bruno, R. Celiberto, C. Gorse, F. Pirani, M. Capitelli, Chem. Phys. Lett. **445**, 133 (2007)
36. M. Capitelli, D. Cappelletti, G. Colonna, C. Gorse, A. Laricchiuta, G. Liuti, S. Longo, F. Pirani, Chem. Phys. **338**, 62 (2007)
37. X. Wang, L. Zhong, Y. Cressault, A. Gleizes, M. Rong, J. Phys. D: Appl. Phys. **47**, 495201 (2014)
38. NIST Computational Chemistry Comparison and Benchmark Database, *NIST Standard Reference Database Number 101*, 2013. http://cccbdb.nist.gov/
39. P. André, W. Bussiére, D. Rochette, Plasma Chem. Plasma Process. **27**, 381 (2007)
40. A.B. Murphy, C.J Arundell, Plasma Chem. Plasma Process. **14**, 451 (1994)
41. F.B.M. Copeland, D.S.F. Crothers, At. Data Nucl. Data Tables **65**, 273 (1997)
42. J.A. Rutherford, D.A.Vroom, J. Chem. Phys. **61**, 2514 (1974)
43. A. Yevseyev, A. Radtsig, B. Smirnov, J. Phys. B: At. Mol. Phys. **15**, 4437 (1982)
44. D. Rapp, W.E. Francis, J. Chem. Phys. **37**, 2631 (1962)
45. E.A. Mason, R.J. Munn, F.J. Smith, Phys. Fluids **10**, 1827 (1967)
46. A.B. Murphy, E. Tam, J. Phys. D: Appl. Phys. **47**, 295202 (2014)
47. A.B. Murphy, Plasma Chem. Plasma Process. **15**, 279 (1995)
48. R.S. Devoto, Phys. Fluids **16**, 616 (1973)
49. C.R. Wilke, J. Chem. Phys. **18**, 517 (1950)
50. J.T. Vanderslice, Stanley Weissman, E.A. Mason, R.J. Fallon, Phys. Fluids **5** (1962)
51. A. Gleizes, Y. Cressault, P. Teulet, Plasma Sources Sci. Technol. **19** (2010)
52. G.E. Palmer, M.J. Wright, J. Thermophys. Heat Tr. **17**, 232 (2003)
53. A. Murphy, J. Phys. D: Appl. Phys. **29**, 1922 (1996)
54. P.C. Stoller, M. Seeger, A.A. Iordanidis, G.V. Naidis, IEEE Trans. Plasma Sci. **41**, 2359 (2013)
55. M. Fang, Q. Zhuang, X. Guo, J. Phys. D: Appl. Phys. **27**, 74 (1994)
56. J. Liu, Q. Zhang1, J.D. Yan, J. Zhong, M.T.C. Fang, J. Phys. D: Appl. Phys. **49**, 435201 (2016)